JAISCR, 2011, Vol.1, No.3, pp. 207–214

CONTROL OF A REDUNDANT 7DOF UPPER-LIMB POWER-ASSIST EXOSKELETON ROBOT

Yoshiaki Hayashi[1], Kazuo Kiguchi[1], Rajiv Dubey[2]

[1]*Department of Advanced Technology Fusion, Saga UniversitySaga 840-8502 Japan*

[2]*Department of Mechanical Engineering, University of South FloridaFL, USA*

Abstract

Many kinds of power-assist robots have been developed in order to assist daily activities or rehabilitation of the elderly or physically weak persons. Upper-limb power-assist robots are important to assist in many daily life activities such as eating, drinking, etc.. A human upper-limb has 7 degrees of freedom to achieve various tasks dexterously. Therefore, to assist all upper-limb joint motions of a human, the upper-limb power-assist robot is required to have 7DOF. To achieve a desired task, a person moves the hand to the desired position and orientation and/or applies certain amount of force to the target. Therefore, it is important that the upper-limb power-assist robots help control the hand position/orientation or hand force of the user. However, the hand position/orientation or hand force is 6-dimensional vector, so the 7DOF upper-limb power-assist robot has a redundancy and in general, a pseudo-inverse matrix is used in the control. In this paper, an optimal control method is proposed to deal with the redundancy of the upper-limb power-assist exoskeleton robot considering comfortable motion of the user. The motion intention and the comfort of the user are taken into account in the pro-posed method. The effectiveness of the proposed method was evaluated by the experiments.

1 Introduction

The increase in the aged population is rapidly progressing in several advanced countries. A shortage of the caregivers for elderly persons is one of the most serious problems. To assist daily life motions of physically weak persons, many kinds of power-assist robots have been developed to assist the daily activities or rehabilitation of physically weak persons such as elderly, disabled, or injured [1]–[11]. The upper-limb power-assist exoskeleton robots [2]–[6] have been getting attention, because the upper-limb motion is important in daily life to carry out various tasks. The upper-limb power-assist robots are supposed to be activated in accordance with user's motion intention in order to assist user's upper-limb motion. For this reason, the biological signals like electromyogram (EMG) are often used so that the power-assist robot can estimate the user's intention in real-time [2], [3].

An upper-limb of a human has 7 degrees of freedom to achieve various tasks dexterously. While an object in 3-dimensional space can be manipulated with 6DOF in general, a human upper-limb has a redundancy and is able to perform dexterous motions such as altering elbow position while keeping the position and the orientation of the hand. Therefore, in order to assist all upper-limb joint motions of a human user, the upper-limb power-assist robot is required to have 7DOF. EMG signal based impedance control has been proposed for the 7DOF upper-limb power-assist exoskeleton robot to control the robot according to the user's motion intention [3]. In this method, the upper-limb power-assist robot focuses on the 6-dimensional hand force vector to es-

timate user's motion intention and assist the estimated motion in real-time. In the controller, the 6-dimensional hand force vector calculated from EMG signals is realized with the impedance control. Because the robot has a redundant degree of freedom, the pseudo-inverse matrix is used in the controller.

Many kinds of motion optimization methods using a pseudo-inverse matrix have been proposed. In reaching motion to move the hand from the initial posture to the target posture for a human upper-limb, Flash et al. proposed the minimum-jerk model [12]. This model is based on the hypothesis that the upper-limb motion is decided so that the hand vector becomes smoother. Uno et al. proposed the minimum torque-change model that considered the physical dynamics of a human [13]. In addition, the methods which optimize the moving distance, the motion energy, etc. have been proposed. There is the method which optimizes the manipulability for a robot also [15]. However, many of these methods only focus on the hand vector. In the upper-limb power-assist exoskeleton robot, it is one of the most important things that the robot follows and assists every joint motion of the user. Specifically, the robot needs to move according to the user's motion intention so that the user can use the robot without the sense of discomfort. This means that the robot needs to assist not only the user's hand motion but also the whole arm motion of user's upper-limb comfortably. In this paper, an optimal control method is proposed to deal with the redundancy of the upper-limb power-assist exoskeleton robot considering comfortable motion of the user. In the proposed control method, not only the user's motion intention of the hand, but also that of the elbow and/or wrist joint is taken into account. The effectiveness of the proposed method was evaluated by the experiments.

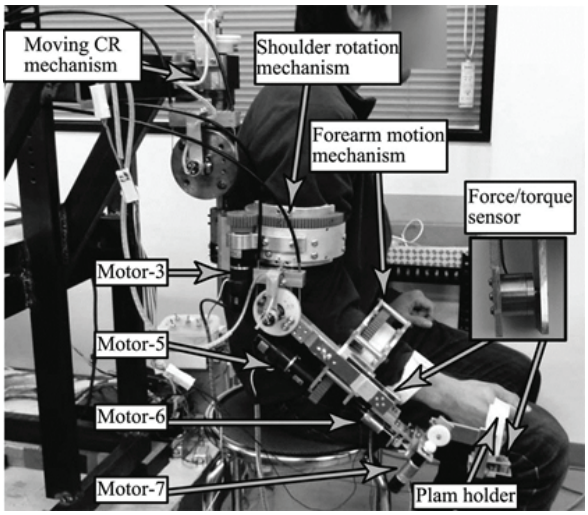

Figure 1. Structure of the robot.

2 7DOF Upper-Limb Power-Assist Exoskeleton Robot [3]

The 7DOF exoskeleton power-assist robot for upper-limb used in this study is shown in Figure 1. The robot consists of seven DC motors with encoders or potentiometers to measure each joint angle, force/torque sensors set in forearm and wrist part to measure the force between the user and the robot and links. The robot is attached to the user with an upper-arm holder, a forearm holder, and a palm holder. This robot is able to assist most of human upper-limb motion (shoulder vertical and horizontal flexion/extension motion, shoulder internal/external rotation motion, elbow flexion/extension motion, forearm supination/pronation motion, wrist flexion/extension motion and wrist radial/ulnar deviation motion). Furthermore, the robot is able to assist combined upper-limb motions such as eating, drinking water and so on in the activities of daily living.

Motor-1, motor-2 and motor-4 are the motors for shoulder vertical, horizontal and elbow motions, respectively. The generated torque by these motors is transferred to the robot joints by pulleys and cable drives. These motors are not installed on the robot directly. Considering the fact that many physically weak persons use wheelchairs, the robot was designed to be installed on a wheelchair. For the safety and the convenience of users, these motors were fixed to the back frame of the wheelchair.

The other four motors are connected to the robot directly by spur gears. Hook-and-loop-fastener parts are used in the three holders (the upper-arm holder, the forearm holder, and the palm holder) for the user to wear the robot.

For shoulder vertical and horizontal motions, a moving center rotation (CR) mechanism has been applied. The main advantage of the CR mechanism is the ability to adjust the distance between the upper-arm holder and the CR of the shoulder joint of the robot in accordance with the shoulder joint angles, in order to cancel out the ill effects caused by the position difference between the CR of the robot shoulder and the human shoulder [2], [3].

Force/torque sensors (PD3-32, NITTA CORPORATION) are installed. The force/torque sensors are used to measure the difference between the motions of a user and the robot.

The safety of the user is the highest priority. Safety components are prepared both in software and hardware to prevent sudden unexpected motion. In the software, maximum torque and maximum velocity are limited. In the hardware, there are physical stoppers for each joint to limit the joint motion within the movable range of human upper-limb. There are also seven switches for each motor near the user so that the user is able to stop the motor immediately in the case of an emergency.

3 EMG-Based Impedance Control

Sixteen channels of EMG signals are used as input signals to estimate the user's motion intention. The locations of EMG electrodes are shown in Figure 2.

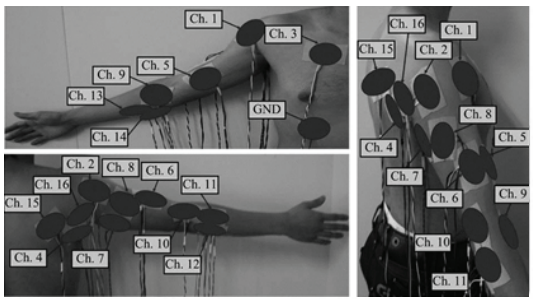

Figure 2. Location of the EMG Electrodes.

Each channel mainly corresponds to one muscle as shown in Table 1, although each motion is related to at least 2 muscles. The control methods (i.e., an EMG-based control method and a force/torque sensor-based control method) are switched automatically according to the user's EMG signal levels [2], [3]. When the user's EMG signal levels are high, EMG-based control is used to control the robot. On the other hand, force/torque sensor-based control is used to control the robot when the user's muscle activation levels are low. The structure of the controller is shown in Figure 3.

Table 1. Muscles for each EMG channel.

EMG channel	Muscle
Ch. 1	Deltoid-anterior
Ch. 2	Deltoid-posterior
Ch. 3	Pectoralis major-clavicular
Ch. 4	Teres major
Ch. 5	Biceps-short head
Ch. 6	Biceps-long head
Ch. 7	Triceps-long head
Ch. 8	Triceps-lateral head
Ch. 9	Pronator teres
Ch. 10	Supinator
Ch. 11	Extensor carpi radialis brevis
Ch. 12	Extensor carpi ulnaris
Ch. 13	Flexor carpi radialis
Ch. 14	Flexor carpi ulnaris
Ch. 15	Infraspinatus
Ch. 16	Teres minor

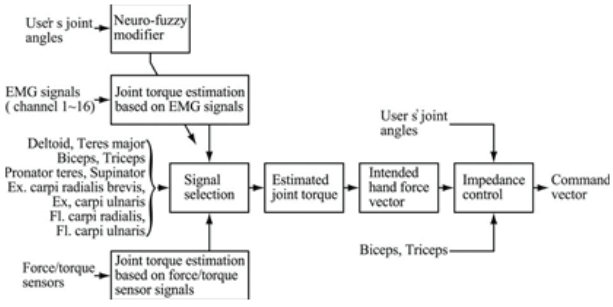

Figure 3. Structure of the Controller [3].

In order to extract the features of the raw EMG signal, the root mean square (RMS) of EMG signal

is calculated and used as an input for the controller. RMS calculation is written as:

$$RMS = \sqrt{\frac{1}{N}\sum_{i=1}^{N} v_i^2} \tag{1}$$

where N is the number of the segments (N=400), v_i is the voltage at ith sampling. The sampling frequency is 2 kHz.

The relationship between the sixteen EMG RMSs and the joint torque vector is able to written as:

$$\tau = \begin{bmatrix} \tau_1 \\ \tau_2 \\ \tau_3 \\ \tau_4 \\ \tau_5 \\ \tau_6 \\ \tau_7 \end{bmatrix} = \begin{bmatrix} w_{11} & w_{12} & \cdots & w_{115} & w_{116} \\ w_{21} & w_{22} & \cdots & w_{215} & w_{216} \\ \vdots & \vdots & \ddots & \vdots & \vdots \\ w_{61} & w_{62} & \cdots & w_{615} & w_{616} \\ w_{71} & w_{72} & \cdots & w_{715} & w_{716} \end{bmatrix} \begin{bmatrix} ch_1 \\ ch_2 \\ \vdots \\ ch_{15} \\ ch_{16} \end{bmatrix} \tag{2}$$

where τ is the joint torque vector, τ_1-τ_7 are the joint torques for motor-1-motor-7, respectively. w_{ij} is the weight value for jth EMG signal to estimate the torque of motor-i and ch_j represents the RMS value of the EMG signal measured in channel i. The weight matrix (i.e., the muscle-model matrix) in the eq. (2) can be defined using the knowledge of human upper-limb anatomy or the results of experiments. Therefore, the joint torque vector generated by muscle force can be calculated if every weight for the EMG signals is properly defined. It is not easy, however, to define the proper weight matrix from the beginning. Furthermore, the posture of the upper-limb affects the relationship between the EMG signals and the generated joint torques because of anatomical reasons such as change of the moment arm.

In other words, the role of each muscle for a certain motion varies in accordance with joint angles. Consequently, the effect of the posture difference of the upper-limb must be taken into account to estimate the correct upper-limb motion for the power assist. Therefore, a neuro-fuzzy muscle-model matrix modifier [3], [14] is applied to take into account the effect of the upper-limb posture difference of the user. The neuro-fuzzy modifier is used to adjust the weight matrix in the eq. (2) by multiplying the coefficients in accordance with the upper-limb posture of the user, so that the effect of upper-limb posture difference can be compensated effectively. It also makes the same effect of adjusting the weight matrix (i.e., the muscle-model matrix) itself to be suitable for each user. The structure of the neuro-fuzzy modifier is the same as a neural network and the process of the signal flow in the neuro-fuzzy modifier is the same as that in fuzzy reasoning as shown in Figure 4. The details of the neuro-fuzzy modifier can be referred in [3], [14].

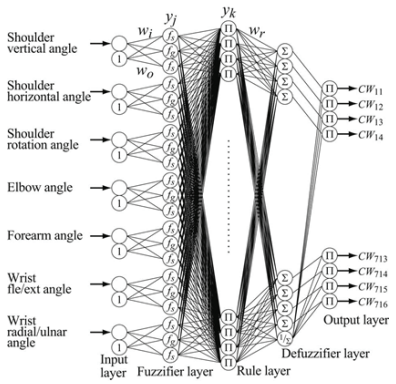

Figure 4. Neuro-fuzzy modifier [3].

To estimate user's motion intention, the hand force vector is calculated. The calculated joint torque vector is transferred to the hand force vector of the user as follows:

$$F_{end} = J^{-T}\tau \tag{3}$$

$$F_{avg} = \frac{1}{N_f}\sum_{i=1}^{N_f} F_{end}(i) \tag{4}$$

$$\ddot{X}_d = M^{-1}F_{avg} \tag{5}$$

where $\boldsymbol{F}_{end}$ is the hand force vector, $\boldsymbol{J}$ is the Jacobian matrix (Since J is not sqauare, a pseudo-inverse needs to be used in eq. (3). This is done later but should be mentioned here), $\boldsymbol{F}_{avg}$ is average of Fend in N_f number of samples, $\ddot{X}_d$is desired hand acceleration vector, and $\boldsymbol{M}$ is the inertia matrix of the user's upper-limb and the robot. Using eq. (5), the following impedance control equation is used to the resultant hand force vector.

$$F = M\ddot{X}_d + B\left(\dot{X}_d - \dot{X}\right) + K\left(X_d - X\right) \tag{6}$$

where $\boldsymbol{F}$ is the resultant hand force vector, $\boldsymbol{B}$ is the viscous coefficient matrix and $\boldsymbol{K}$ is the spring coefficient matrix. Finally, the joint torque command vector is calculated as follows.

$$\tau_{motor} = \kappa J^{\mathrm{T}} F \tag{7}$$

where τ_{motor} is the joint torque command vector and κ is the power-assist rate.

Since the effect of the upper-limb posture change on each impedance coefficient is nonlinear, fuzzy reasoning is applied to estimate the effect of the posture on each impedance coefficient [3].

4 Motion Optimization Using Pseudo-Inverse Matrix

The Jacobian matrix $\boldsymbol{J}$ is used in the controller. Although the robot has 7 motors, the hand force vector is a 6-dimensional vector. Therefore, a pseudo-inverse matrix must be used for $\boldsymbol{J}^{-1}$ since $\boldsymbol{J}$ is a 6×7 matrix. The assist motion is optimized for the power-assist robot using a pseudo-inverse matrix considering the user's motion intention of the elbow and/or wrist joint. Many optimization methods using a pseudo-inverse matrix have been already proposed [12][13][15]. For example, the methods which optimize the moving distance, the motion energy, *etc*. have been proposed. In addition, there is the method which optimizes the manipulability for a robot. In the upper-limb power-assist exoskeleton robot, it is the most important that the robot follows and assists every joint motion of the user. Specifically, the robot needs to move according to the user's motion intention so that the user can use the robot without the sense of discomfort. This means that the robot needs to follow not only the user's hand motion but also the whole joint motion of user's upper-limb comfortably. The hand force vector $\boldsymbol{F}_{end}$ in eq. (3) is rewritten as follows:

$$F_{end} = J^{+T}\tau + (I_6 - J^{+}J)\eta \tag{8}$$

where $\boldsymbol{J}^{+T}$ is the transpose of the pseudo-inverse matrix of $\boldsymbol{J}$, ($\boldsymbol{I}_6$ - $\boldsymbol{J}^{+}\boldsymbol{J}$)$\eta$ represents the null space and η is an arbitrary vector. $\boldsymbol{F}_{end}$ in eq. (3) is hand force vector at the case of $\eta = \boldsymbol{0}$. In this paper, η is decided based on the intended wrist motion vector from the elbow joint and/or elbow motion vector from the shoulder joint by the user. The intended wrist motion vector and the elbow motion vector are estimated based on the EMG signals also.

The coordinate frame Σ_0, Σ_s and Σ_e are defined as shown in Figure 5.

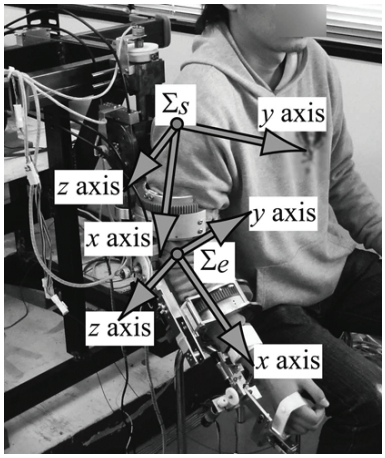

Figure 5. Coordinate frames.

Σ_0 is the fixed coordinate on the robot. Σ_s is the moving coordinate frame fixed on the shoulder joint. x axis is the shoulder internal/external rotation axis, y axis is the shoulder horizontal flexion/extension axis and z axis is the shoulder vertical flexion/extension axis in Σ_s. Σ_e is the moving coordinate frame fixed on the elbow joint. x axis is the forearm pronation/supination axis and z axis is the elbow flexion/extension axis in Σ_e. x_e, y_e, and z_e are the position of Σ_e origin in Σ_s. Then, the robot does not generate the force along x_e, and the moments about y_e and z_e because of the mechanical limitation. So the force vector for the elbow motion is defined as $\boldsymbol{F}_{elbow} = [f_y\ f_z\ n_x]^T$ and calculated as follows based on eq. (3).

$$F_{elbow} = J_e^{-T}\tau_e \tag{9}$$

where f_y and f_z are the forces along y_e and z_e, respectively. $\tau_e = [\tau_1\ \tau_2\ \tau_3]^T$ is the joint torques calculated in eq. (2). $\boldsymbol{J}_e$ is the 3×3 Jacobian matrix from the shoulder joint to elbow joint. Using the same calculation procedure from eq. (4) to eq. (5), the following desired acceleration vector of the elbow is obtained as:

$$\ddot{X}_{e,d} = M_e^{-1}F_{e,avg} \tag{10}$$

where $\boldsymbol{F}_{e,avg}$ is the average of $\boldsymbol{F}_{elbow}$ in N_f number of samples, $\ddot{X}_{e,d}$is the desired acceleration vector at the elbow joint and $\boldsymbol{M}_e$ is the weight matrix of the upper-limb from the shoulder to elbow. Then, the cost function for the elbow motion is decided as follows:

$$E_e = \frac{C_e}{\left\langle \left(\ddot{X}_{e,d} - \ddot{X}\right), \left(\ddot{X}_{e,d} - \ddot{X}\right)\right\rangle + 1} \tag{11}$$

where E_e is the cost function and C_e is a constant value for the estimated elbow motion effect. If E_e is near to the maximum, it means that the elbow's acceleration becomes closer to the desired acceleration. Using E_e, the element of η_e is represented as the following equation.

$$\eta_{e,i} = k_e \frac{\partial E_e}{\partial \theta_i} \quad (i = 1-7) \tag{12}$$

where k_e is the constant coefficient.

The force vector for the wrist motion is defined as $\boldsymbol{F}_{wrist} = [n_x\ n_y\ n_z]^T$. $\tau_w = [\tau_5\ \tau_6\ \tau_7]^T$ is the joint torques calculated in eq. (2). $\boldsymbol{J}_w$ is the 3×3 Jacobian matrix from the elbow joint to wrist joint (orientation only). The desired acceleration vector of the wrist is obtained as:

$$F_{wrist} = J_w^{-T} \tau_w \tag{13}$$

The following desired acceleration vector of the wrist is obtained as:

$$\ddot{X}_{w,d} = M_w^{-1} F_{w,avg} \tag{14}$$

where $\boldsymbol{F}_{w,avg}$ is the average of $\boldsymbol{F}_{wrist}$ in N_f number of samples.

The cost function for the wrist motion is decided as follows:

$$E_w = \frac{C_w}{\left\langle \left(\ddot{X}_{w,d} - \ddot{X}\right), \left(\ddot{X}_{w,d} - \ddot{X}\right) \right\rangle + 1} \tag{15}$$

where E_w is the cost function and C_w is a constant value for the estimated wrist motion effect. If E_w is near to the maximum, it means that the wrist's acceleration becomes closer to the desired acceleration. Using E_w, the element of η_w is represented as the following equation.

$$\eta_{w,i} = k_w \frac{\partial E_w}{\partial \theta_i} \quad (i = 1-7) \tag{16}$$

where k_w is the constant coefficient.

Using E_e and E_w, the element of η is written as:

$$\eta_i = k_e \frac{\partial E_e}{\partial \theta_i} + k_w \frac{\partial E_w}{\partial \theta_i} \quad (i = 1-7) \tag{17}$$

Here, k_w is basically defined as (1-k_e). If only the elbow motion intention of the user is taken into account, k_e is defined as 1 and k_w is defined as 0 and vice versa. By using eqs. (8), (17), and (4)-(7), the joint torque command vector τ_{motor} is obtained.

5 Experiments

In order to evaluate the effects of the proposed motion optimization method, two types of experiments were carried out. In these experiments, three healthy young male subjects performed the upper-limb combined motions. The power-assist rate was set to be 1.4. The first experiment was performed to evaluate the effectiveness of the proposed motion optimization method over the conventional method using eq. (3). In this experiment, the subject is supposed to pour water into a cup on a table from a grasped plastic bottle as shown in Figure 6.

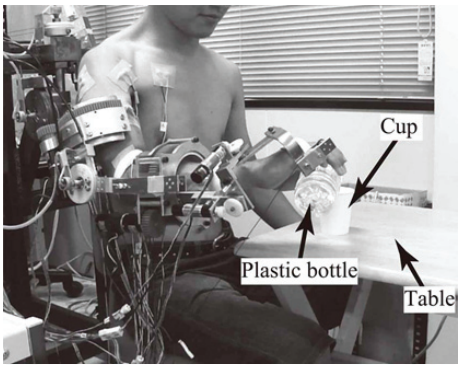

Figure 6. First experiment.

The weight of the plastic bottle was 0.5kg and the height of the table is 670mm. Since the wrist motion of the user is important in this experiment, k_e and k_w in eq. (17) are set to be 0.0 and 1.0, respectively. The experimental results with the conventional method are shown in Figure 7 and those with the proposed method are shown in Figure 8.

In Figures 7 and 8, (a) shows the hand position, (b) shows EMG signals and (c) shows the motor input voltage.

The experimental results shown in Figure 8 shows that the wrist motion (motor-7: wrist radial/ulnar deviation motion) of the user is assisted well and the amount of EMG signals (ch.12: Extensor carpi ulnaris) is smaller than that shown in Figure 7, although the hand motions are almost the same. These results show that the intended wrist motion of the user is moderately realized by the proposed method.

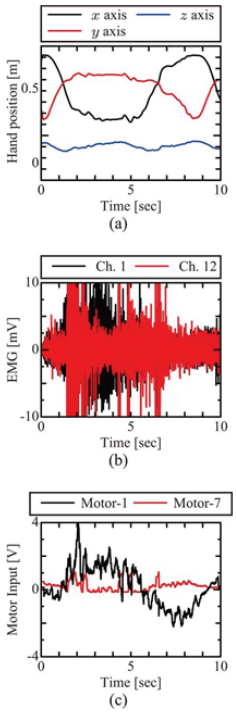

Figure 7. Experimental result without the proposed method.

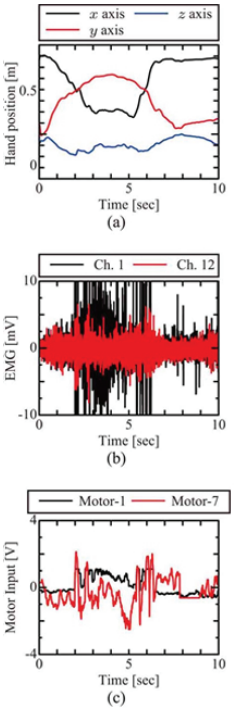

Figure 8. Experimental result with the proposed method.

The second experiment was performed to evaluate the effectiveness of the generated elbow and wrist motion. In this experiment, the subject is supposed to move the filled plastic bottle with water onto the rack as shown in Figure 9.

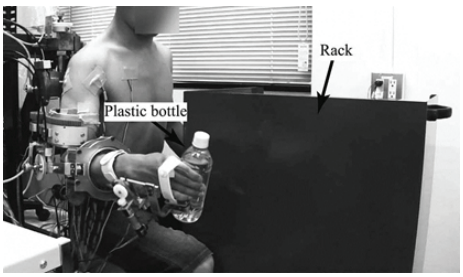

Figure 9. Second experiment.

The weight of the plastic bottle was 0.5kg and the height of the rack is 880mm. In this experiment, two kinds of upper-limb motions were performed. One was the motion that the shoulder joint was mainly activated on purpose. Figures 10 shows the experimental results when k_e and k_w in eq. (17) were defined as 0.8 and 0.2, respectively. The other was the motion that the wrist joint was mainly activated on purpose. Figures 11 shows the experimental results when k_e and k_w in eq. (17) were defined as 0.2 and 0.8, respectively.

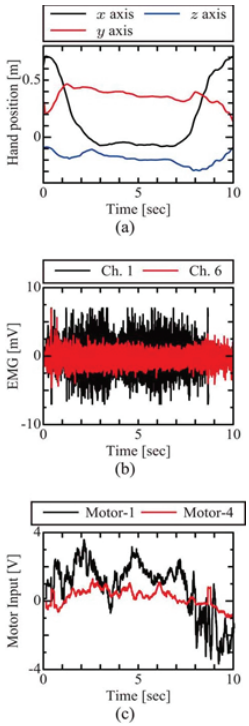

Figure 10. Second experimental result with the proposed method.

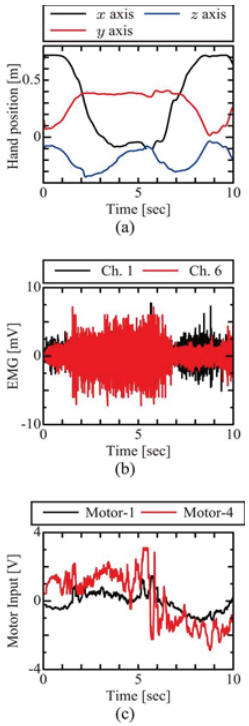

Figure 11. Second experimental result with the proposed method.

In Figures 10 and 11, (a) shows the hand position, (b) shows EMG signals and (c) shows the motor input voltage. In Figure 10, the elbow motion (motor-1: shoulder vertical flexion/extension motion) was actively assisted. On the other hand, the wrist motion (motor-4: elbow flexion/extension motion) was actively assisted in Figure 11. These experiment results show that the intended elbow motion or wrist motion can be realized by the proposed method. As shown in these experimental results, the generated assist motion with the existing method might not always reflect the user's motion intention at the joint level. On the other hand, the generated assist motion with the proposed optimization method reflects the user's motion intention in the elbow motion or the wrist motion as well as the hand motion.

6 Conclusion

In order to assist all 7DOF upper-limb joint motions of a physically weak person, the upper-limb power-assist exoskeleton robot is required to have the same number of DOF or more. Since the 7DOF upper-limb power-assist robot is a redundant robot, null space should be effectively utilized. In this paper, the motion optimization method for the 7DOF upper-limb power-assist robot is proposed. The proposed method focuses on the elbow motion and the wrist motion to realize the user's intention by using null space of a pseudo-inverse matrix. The effectiveness of the proposed method was evaluated by the experiments. The experimental results show that the control with the proposed method reflects the user's intention at the elbow and wrist compare to the control with the existing method.

References

[1] E. Guizzo E. and H. Goldstein, *The Rise of the Body Bots*, IEEE Spectrum, vol.42, no.10, 2005, pp.42-48.

[2] K. Kiguchi, T. Tanaka and T. Fukuda, *Neuro-Fuzzy Control of a Robotic Exoskeleton with EMG Signals*, IEEE Trans. on Fuzzy Systems, vol.12, no.4, 2004, pp.481-490.

[3] R.A.R.C. Gopura and K. Kiguchi, *SUEFUL-7: A 7DOF Upper-Limb Exoskeleton Robot with Muscle-Model-Oriented EMG-Based Control*, Proc. of IEEE/RSJ International Conf. on Intelligent Robots and Systems, 2009, pp.1126-1131.

[4] J. C. Perry et al., *Upper-Limb Powered Exoskeleton Design*, Trans. on Mechatronics, vol.12, no.4, 2007, pp.408-417.

[5] J. L. Pons, et al., *Upper-Limb Robotic Rehabilitation Exoskeleton: Tremor Suppression,* Rehabilitation Robotics, Book edited by S. S. Kommu, 2007, pp.453-470.

[6] N.G. Tsagarkis and D.G. Caldwell, *Development and Control of a 'Soft-Actuated' Exoskeleton for Use in Physiotherapy and Training*, Autonomous Robots, vol.15, no.3, 2003, pp.21-33.

[7] A.B. Zoss, H. Kazerooni, and A. Chu, *Biomechanical Design of the Berkeley Lower Extremity Exoskeleton (BLEEX),* IEEE/ASME Transactions on Mechatronics, vol.11, no.2, 2006, pp. 128-138.

[8] S. Lee and Y. Sankai, *Power Assist Control for Walking Aid with HAL-3 Based on EMG and Impedance Adjustment around Knee Joint,* Proc. of IEEE/RSJ International Conf. on Intelligent Robots and Systems, 2002, pp.1499-1504.

[9] K. Nagai and I. Nakanishi, *Force Analysis of Exoskeletal Robotic Orthoses for Judgment on Mechanical Safety and Possibility of Assistance*, Journal of Robotics and Mechatronics, vol.16, no. 5, 2004, pp.473-481.

[10] L. Lucas, M. DiCicco, and Y. Matsuoka, *An EMG-Controlled Hand Exoskeleton for Natural Pinching*, Journal of Robotics and Mechatronics, vol.16, no. 5, 2004, pp.482-488.

[11] J. Rosen, M. Brand, M. Fuchs, and M. Arcan, *A Myosignal-Based Powered Exoskeleton System*, IEEE Trans. on System Man and Cybernetics, Part A, vol.31, no.3, 2001, pp. 210-222.

[12] T. Flash and N. Hogan, *The coordination of arm movements: An experimentally confirmed mathematical model*, Journal of Neuroscience, vol.5, no.7, 1985, pp.1688-1703.

[13] Y. Uno, M. Kawato, and R. Suzuki, *Formation and control of optical trajectory in human multi-joint arm movement - minimim torque-change model*, Biological Cybernetics, 61, 1989, pp.89-101.

[14] K. Kiguchi and Q. Quan, *Muscle-Model-Oriented EMG-Based Control of an Upper-Limb Power-Assist Exoskeleton with a Neuro-Fuzzy Adjuster*, Proc. of IEEE World Congress of Computational Intelligence, 2008, pp.1179-1184.

[15] L. Sciavicco and B. Siciliano, *Modeling and Control of Robot Manpulators*, McGraw Hill Co., 1996.